Solar Phys (2019) 294:134
https://doi.org/10.1007/s11207-019-1518-3

Are Solar Energetic Particle Events and Type II Bursts Associated with Fast and Narrow Coronal Mass Ejections?

S.W. Kahler[1] · A.G. Ling[2] · N. Gopalswamy[3]

Received: 28 February 2019 / Accepted: 29 August 2019

Abstract Gradual solar energetic ($E > 10$ MeV) particle (SEP) events and metric through kilometric wavelength type II radio bursts are usually associated with shocks driven by fast ($V \geq 900$ km s^{-1}) and wide ($W \geq 60°$) coronal mass ejections (FW CMEs). This criterion was established empirically by several studies from solar cycle 23. The characteristic Alfvén speed in the corona, which ranges over 500 – 1500 km s^{-1} at heights ≥ 2 R_o, provides the minimum V requirement for a CME to drive a shock, but the general absence of SEP events or type II bursts with fast and narrow ($W < 60°$) CMEs has not been explained. We review and confirm the earlier studies with a more comprehensive comparison of SEP events and type II bursts with fast and narrow (FN) CMEs. We offer an explanation for the lack of SEP event and type II burst associations with FN CMEs in terms of recent heuristic arguments and modeling that show that the response of a magnetized plasma to the propagation of a CME depends on the CME geometry as well as on its speed. A clear distinction is made between a projectile that propagates through the medium to produce a bow shock, and a 3D piston that everywhere accumulates material to produce a broad shock and sheath. The bow shock is unfavorable for producing SEP events and type II bursts, but the 60° cut-off is not explained.

Keywords Sun: coronal mass ejections (CMEs) · Sun: radio radiation · Sun: particle emission · Shock waves

1. Introduction

There are two classes of solar energetic ($E \geq 10$ MeV nuc^{-1}) particle (SEP) events, known as gradual and impulsive, whose differences and properties have been described by

✉ S.W. Kahler
stephen.kahler@us.af.mil

1 Air Force Research Laboratory, Space Vehicles Directorate, 3550 Aberdeen Ave., Kirtland AFB, NM 87117, USA

2 Atmospheric Environmental Research, Albuquerque, NM 87110, USA

3 Laboratory for Solar Physics, NASA Goddard Space Flight Center, Greenbelt, MD 20771, USA

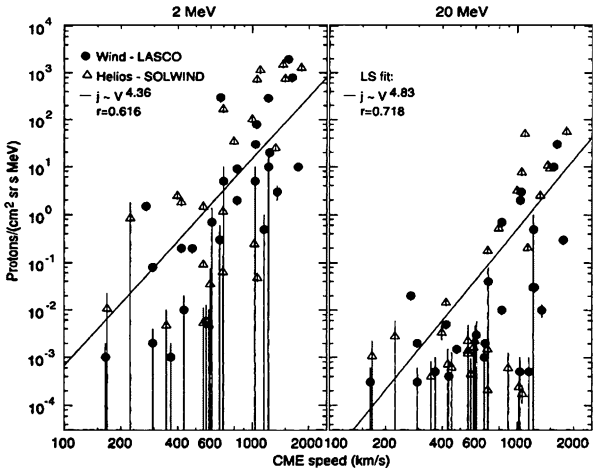

Figure 1 Correlations of peak proton intensities at ≈ 2 MeV (*left*) and ≈ 20 MeV (*right*) with CME speed for two different data sets. Reproduced from Reames (2000, 2017) with permission of the author.

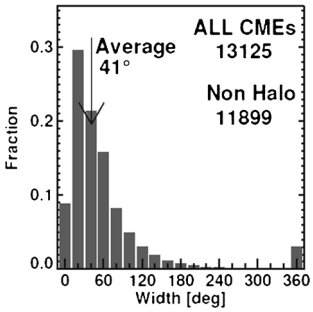

Figure 2 CME width distribution compiled by Gopalswamy *et al.* (2010). Halo CMEs are those of full 360° widths. Reproduced with permission of the author.

Reames (2013, 2017). Gradual SEP events, lasting several days, are produced in coronal-interplanetary shocks driven by fast ($V_{\rm CME} \geq 900$ km s^{-1}) coronal mass ejections (CMEs). They are associated with type II radio bursts, long-duration eruptive soft X-ray and Hα flares and extend over broad longitude ranges relative to their associated flare locations, sometimes beyond the east or west solar limbs. Their elemental abundances are similar to coronal abundances (Schmelz *et al.*, 2012).

The correlation of CME speeds $V_{\rm CME}$ with $E \geq 10$ MeV SEP event peak intensities (Figure 1) has long been known (Reames, 2000) and often validated (*e.g.*, Gopalswamy *et al.*, 2003; Kahler and Vourlidas, 2005; Park, Moon, and Gopalswamy, 2012; Miteva *et al.*, 2013; Richardson *et al.*, 2014; Dierckxsens *et al.*, 2015; Takahashi, Mizuno, and Shibata, 2016). The basic paradigm is that CMEs with $V_{\rm CME} > V_{\rm f}$, the plasma fast-mode speed, drive shocks that can accelerate seed particles to the high energies observed as SEP events in space. Various models of $V_{\rm f}$ (Gopalswamy *et al.*, 2001a), or of $V_{\rm a}$, the Alfvén speed (Guhathakurta, Sittler, and McComas, 1999; Mann *et al.*, 2003; Evans *et al.*, 2008), *versus* coronal height R in active regions or streamers generally place peak values at $3-8\ R_{\rm o}$ and show $V_{\rm f} < 500$ km s^{-1} above 10 $R_{\rm o}$.

Physical properties of CMEs, observed over several decades by a series of coronagraphs, have been summarized by Webb and Howard (2012). Angular widths W, measured in projection against the sky plane, define one of their fundamental properties. The average W determined from the statistical distribution of the 13 125 CMEs (Figure 2) reported to date in a catalog (Gopalswamy *et al.*, 2009a) for the SOHO/LASCO mission was 41° (Gopal-

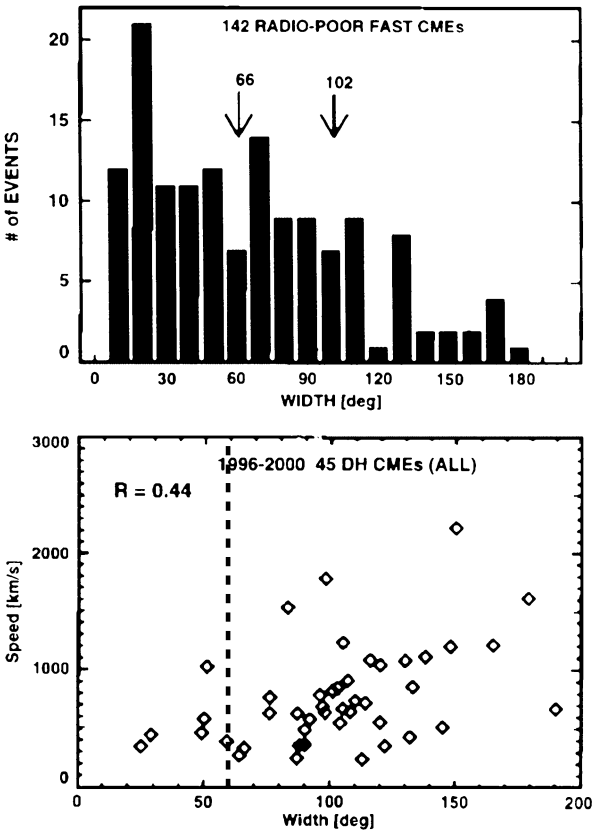

Figure 3 *Top*: Width distribution of radio-poor CMEs with $V_{CME} > 900\ km\,s^{-1}$. *Bottom*: Speed and width distribution of DH CMEs. Halo CMEs are not included. *Dashed line* indicates 60°. Adapted from Gopalswamy *et al.* (2001b) and reproduced by permission of the AGU.

swamy *et al.*, 2010), comparable to those observed with earlier coronagraphs (Webb and Howard, 2012).

In the first study to determine the properties of CMEs associated with decametric–hectometric (DH) type II bursts Gopalswamy *et al.* (2001b) found associations increasing with faster and wider CMEs. They noted that even among the fastest ($V_{CME} \geq 900\ km\,s^{-1}$) CMEs there was a large population of radio-poor narrow CMEs (Figure 3). Only six of the 101 DH type II bursts of the study had widths $W < 60°$. The average 66° width of radio-poor CMEs was much smaller than the average 102° width of the radio-rich sample.

An early study by Kahler and Reames (2003) to determine 20-MeV proton SEP event associations with fast ($V_{CME} \geq 900\ km\,s^{-1}$) CMEs at longitudes from W30° to behind the west limb found only a single event with $W < 60°$ (Figure 4), and that event was a known impulsive (Kahler, Reames, and Sheeley, 2001), not gradual, SEP event. All 23 of the fast CMEs with $W < 60°$ were not associated with gradual SEP events. Thus, the general lack of fast ($V_{CME} > 900\ km\,s^{-1}$) and narrow ($W < 60°$) (FN) CME associations now included both DH type II bursts and gradual SEP events. With a larger statistical base of SOHO/LASCO CMEs from 1996 to 2005 Gopalswamy *et al.* (2008b) extended the CME statistical comparisons with DH type II bursts and GOES $E > 10$ MeV events of at least 1 pfu (proton flux unit, 1 pfu = 1 proton $cm^{-2}\,s^{-1}\,sr^{-1}$). Their results (Figure 5) confirmed the earlier work and established the FW CMEs as the causes of type II radio bursts and SEP events (Gopalswamy, 2008). Exceptional CMEs with $V_{CME} = 400\ km\,s^{-1}$ and an associated type II burst

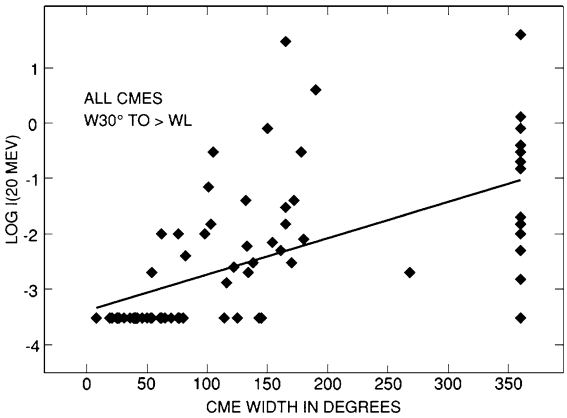

Figure 4 Plot of logs of 20-MeV event peak intensities *versus* CME widths for 75 CMEs with sources from W30° to behind the west limb. All CME speeds are $V_{\mathrm{CME}} > 900\ \mathrm{km\,s^{-1}}$. The *diagonal line* is the least-squares best fit, and only one event has $W < 60°$. Figure 5 of Kahler and Reames (2003). Reproduced by permission of the AAS.

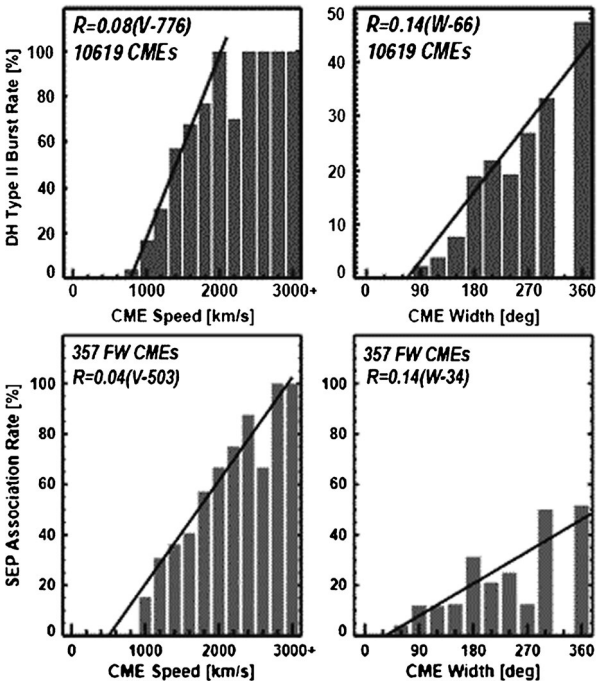

Figure 5 *Top*: Association rates of DH type II bursts as functions of CME speed and width for all CMEs observed from 1996 to 2005. *Bottom*: Same for $E > 10$-MeV SEP events of ≥ 1 pfu, but now for only FW CMEs. From Gopalswamy *et al.* (2008a). Reproduced by permission of the AAS.

and/or SEP event, or FW CMEs with no such associations (Gopalswamy *et al.*, 2008a,b), can be attributed to variations of V_{a} in different types of coronal structures traversed by the CMEs.

The simple explanation of deviations of V_{CME} from a strict requirement of $V_{\mathrm{CME}} > 900\ \mathrm{km\,s^{-1}}$ for DH type II burst or SEP event associations is not matched by a similar conceptual understanding of why FN CMEs seem to be excluded from those associations. FN CMEs also exceed the average coronal V_{a} and should often produce shocks, as do the FW CMEs. We (Kahler and Gopalswamy, 2009) briefly reviewed this question and offered an explanation in terms of two kinds of shocks produced by projectiles and pistons, which we associate with the FN and FW CMEs, respectively. Here we will confirm these CME

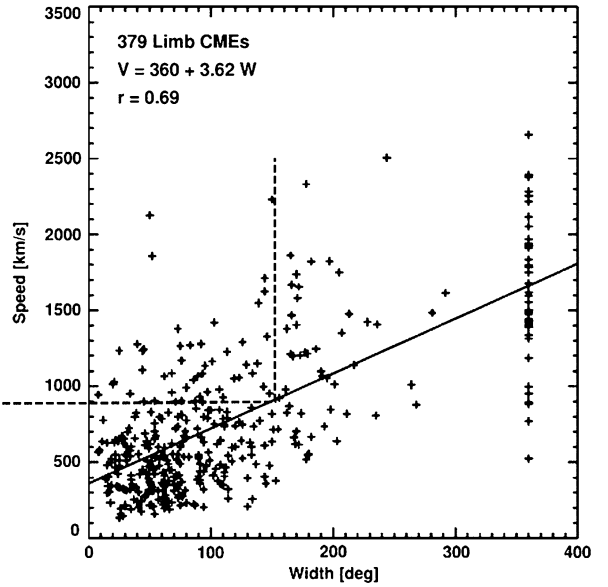

Figure 6 Speed–width distribution of limb CMEs with central meridian distance (CMD) between W60° and W90°, with halo CMEs plotted at 360°. *Diagonal line* is the least-squares best fit. *Dashed lines* are lower (upper) limits of the speed (width) CMEs selected from the LASCO catalog for the comparisons with metric type II bursts and SEP events. Adapted from Gopalswamy *et al.*, 2009b. Reproduced with permission of the authors.

associations with more extensive and recent data sets and with the same basic explanation explore the question more broadly.

2. Data Analysis

For our analysis we want to select FN CMEs in the LASCO CDAW catalog (Gopalswamy *et al.*, 2009a) through July 2016. The plot of Figure 6 shows an early V–W distribution of limb CMEs compiled by Gopalswamy *et al.* (2009b). Our first selection cut is only fast (linear first-order $V_{\rm CME} \geq 900$ km s^{-1}) CMEs above the horizontal dashed line, and the second is widths $10° \leq W \leq 150°$ shown by the vertical dashed line. We do not include the narrowest ($W < 10°$) CMEs, whose CDAW numbers increased after 2004 due to observer bias (Webb and Howard, 2012) and are lower than those of the alternative CACTus catalog (Yashiro, Michalek, and Gopalswamy, 2008; Robbrecht, Berghmans, and Van der Linden, 2009). The extension of W to 150° allows comparison of FN CME properties with those of the broader ($60° < W \leq 150°$) CMEs. We further restrict the selection to $200° <$ PA (position angle) $< 340°$, limiting the CMEs to those of the west limb, which would be more favorable for SEP event associations. Unlike the CMEs of Figure 6, our total sample of 232 CMEs will also include a large number of CMEs behind the limb. We find a weak Pearson CC (correlation coefficient) = 0.20 between the speeds $V_{\rm CME}$ and widths W of the 232 sample CMEs, as might be expected from Figure 6. The LASCO CDAW catalog gives CME linear speeds and 2nd-order speeds at final heights based on fits to the CME height–time profiles. We also looked at differences between those two speeds and found similar median values of -52 km s^{-1} for FN CMEs and -67 km s^{-1} for those with $W > 60°$. Thus we do not find the sample CMEs to be distinguished from larger statistical samples.

2.1. Type II Bursts

For our comparison of FN CMEs with type II bursts, we use a comprehensive listing of 1190 metric type II bursts (S.M. White, priv. comm.) reported through July 2016 by the Culgoora

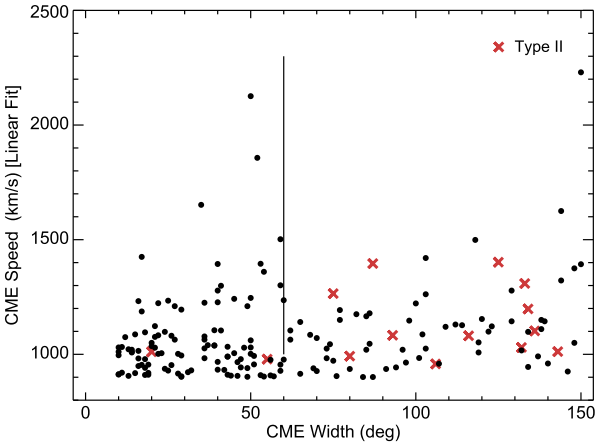

Figure 7 Plot of CMEs with $V_{CME} \geq 900$ km s^{-1} showing those associated with metric type II bursts. There are only three CMEs in the FN ($W < 60°$, *vertical line*) range, and only one, on 2002 October 20 at 1430 UT, with $W < 50°$.

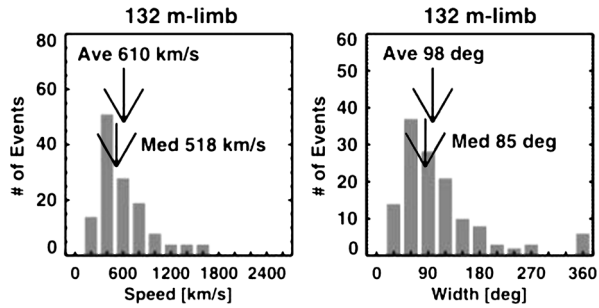

Figure 8 *Left*: the speed distribution of 132 CMEs near ($< 30°$) the limb associated with metric type II bursts. *Right*: the width distribution of the same CMEs. Extracted from Figure 4 of Gopalswamy *et al.* (2005). Reproduced by permission of the AGU.

(Labrum, 1972) and Radio Solar Telescope Network (RSTN) (San Vito, Learmonth, Sagamore Hill (Guidice, 1979), and Palahua) observatories. For associated events, the type II onset times generally preceded the first associated CME observation in the LASCO C2 coronagraph by up to 30 minutes. The resulting speed–width distribution of CMEs is shown in Figure 7, where red crosses indicate the associated type II bursts. Among the 129 FN CMEs are found only three type II bursts, while 14 type II bursts occur among the 103 wider ($60° < W \leq 150°$) CMEs. We note that there may be type II burst associations to be found among narrow CMEs of slower ($V_{CME} < 900$ km s^{-1}) speeds, but we are here selecting on FN CMEs likely to exceed the local V_a speeds. An earlier comparison by Gopalswamy *et al.* (2005) of CMEs with Hα flare sources within 30° of the limb and associated with metric, but not DH, type II bursts, yielded median speeds and widths of only 518 km s^{-1} and 85°, respectively, when halo CMEs were excluded from the comparisons (Figure 8). Thus, their work would not suggest the relative deficit of metric type II burst associations we find here for the FN CMEs.

2.2. SEP events

We compare our FN CME list with two recent compilations of SEP events. The first is a list of 217 *Wind*/EPACT 20-MeV proton events associated with CMEs from 1996 through 2008 by Kahler (2013). The plot in Figure 9 shows the subset of 183 CMEs through 2008 with $V_{CME} \geq 900$ km s^{-1}. Only two of the 110 FN CMEs were associated with 20-MeV proton events, and again, that included the impulsive 2000 May 1 event (Kahler, Reames,

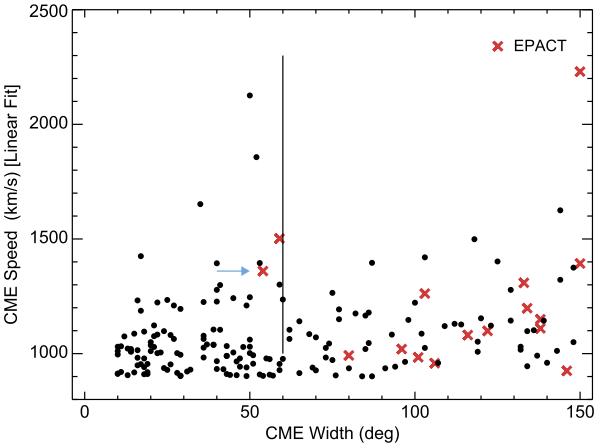

Figure 9 Plot of EPACT 20-MeV proton events (Kahler, 2013) associated with CMEs of $V_{CME} \geq 900$ km s^{-1}, indicated with *red crosses*. There were 183 selected CMEs during the 1996 – 2008 period of the EPACT events. FN CMEs lie *left* of the vertical line. The *blue arrow* points to the impulsive event of 2000 May 1.

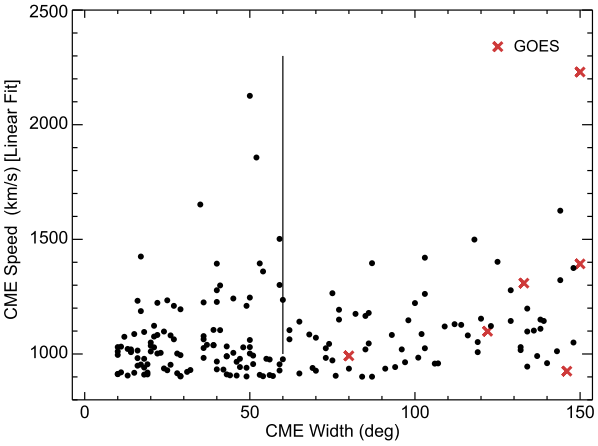

Figure 10 Plot of GOES $E > 10$ MeV proton events (Kahler and Ling, 2019) associated with 248 CMEs of $V_{CME} \geq 900$ km s^{-1}, indicated with *red crosses*. FN CMEs lie *left* of the vertical line. All seven of the proton events were associated with CMEs of $W > 60°$.

and Sheeley, 2001). Of the remaining 73 CMEs with $60° < W \leq 150°$ there are 16 EPACT 20-MeV proton events.

We take as a second list of SEP events the GOES $E > 10$ MeV events of ≥ 1.2 pfu from 1998 through 2016 compiled by Kahler and Ling (2019). A number of events are common to the two lists, but the GOES energy and intensity dynamic ranges are lower than those of the EPACT events. No GOES $E > 10$ MeV events are found among the 129 FN CMEs (Figure 10), while seven of the 103 wider (61° – 150°) have SEP event associations.

These metric type II burst and SEP event comparisons with a comprehensive list of 232 LASCO fast CMEs clarify the earlier results of an essential cut-off at $W = 60°$ reported by Gopalswamy *et al.* (2001a,b) for DH type II bursts and by Kahler and Reames (2003) for SEP events. The $V_{CME} \geq 900$ km s^{-1} speeds of the FN CMEs should easily exceed the V_a or V_f coronal speeds needed to drive shocks and accelerate SEPs. There is clearly another requirement or condition for shocks and SEPs that the FN CMEs do not meet. We suggest a possible solution to this question in the next section.

3. Results and Discussion

When large numbers of CME observations became available from LASCO, there were attempts to model the forces that controlled the propagation of CMEs through the solar wind (SW). The dynamics of CMEs in the SW has generally been treated in terms of drag forces acting on a magnetic structure plowing through the SW. Cargill and Schmidt (2002) and Cargill (2004) modeled cylindrically symmetric CMEs moving magnetohydrodyamically through the SW, and Vršnak *et al.* (2004), Vršnak, Vrbanec, and Čalogovi (2008) calculated drag forces based on extensive observations of CME propagation. Drag forces varied with CME speed, height, and effective CME area and inversely with CME mass, but the CMEs were treated as cylindrically symmetric structures with SW flowing past the CME. Recently Dumbović *et al.* (2018) used a drag-based ensemble model for CME propagation. Russell and Mulligan (2002a,b) considered the shapes of bow shocks preceding interplanetary CMEs (ICMEs). For a symmetric flux-rope ICME they invoked two radii of curvature, one corresponding to the cross section and the other to the curvature of the flux-rope axis. The basic bow shape for a shock was also invoked by Russell and Jian (2008) for a general comparison of ICMEs with magnetospheres.

CME-driven shocks can be described by two fundamentally different processes. The first is the familiar bow shock, formed as SW flows around a relatively narrow projectile, and the second is an expansion shock, formed ahead of a piston driver expanding outward through and accreting the SW. While the projectile-driven bow shock has been the dominant model for understanding fast CMEs, the possible application to CMEs of the alternative piston-driven or "snow plough" model was suggested by Tappin (2006), and the two models were contrasted qualitatively in a review of coronal shock waves by Vršnak and Cliver (2008). Appreciating this fundamental difference of the two models, Takahashi and Shibata (2017) introduced an analytic "sheath-accumulating propagation" model, similar to the piston-driven model.

Insightful model comparisons of the two kinds of shock sheaths were carried out by Siscoe and Odstrcil (2008). One difference is that the calculated shock stand-off distance is smaller for the expansion shock than for the bow shock when normalized to the same radius of curvature of the driver. Figure 11 compares the two shock stand-off distances for a ratio of specific heats of $\gamma = 5/3$. Since the projectile magnetosphere is assumed to have a fixed size, the stand-off distance in a uniform medium is also fixed, but the shock stand-off distance continually grows as the size of the expanding ICME increases by accreting the SW. An important factor is that the ICME is expanding within an outflowing SW, so that the azimuthal expansion speed is always greater than the radial speed of the ICME front relative to the SW flow (Siscoe and Odstrcil, 2008). Takahashi and Shibata (2017) also make this point, that if the sheath thickness is not comparable to or larger than the lateral extent of the CME, the model breaks down because plasma escapes around the sides of the CME (Figure 11).

More detailed calculations of ICME expansion shocks by Žic *et al.* (2008) show that shock formation times and stand-off distances are shorter for: i) higher $V_{\rm CME}$, ii) higher CME accelerations, and iii) larger Alfvén Mach numbers $M_{\rm a}$, and longer for: i) longer acceleration phase durations and ii) higher ambient $V_{\rm a}$.

White-light structures observed ahead of CMEs have been confirmed by various authors (Vourlidas *et al.*, 2003; Kahler and Vourlidas, 2005; Gopalswamy and Yashiro, 2011; Lee *et al.*, 2014) to be driven fast-mode shocks. The choice between a piston-driven or bow shock interpretation has not been clear, however. Ontiveros and Vourlidas (2009) modeled all their 13 FW CME-driven shocks in terms of the bow shock. Kwon, Zhang, and Olmedo

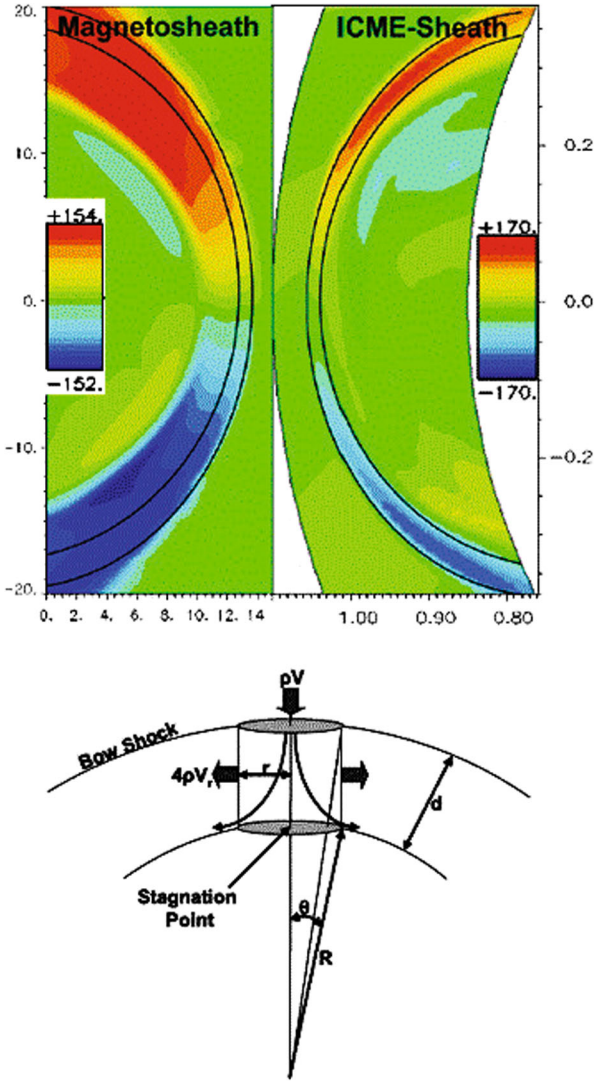

Figure 11 *Top*: Comparison of azimuthal color-coded flow speeds in shock sheaths around a magnetospheric bow shock (*left*) and an ICME piston-driven shock (*right*), both scaled to a common radius of curvature of the shock driver. The matching curved lines show that the sheath thickness of the bow shock is more than twice that of the piston shock. *Bottom*: Schematic to illustrate that all material flowing into the bow shock is compressed and deflected to flow around the driver, as indicated in the *left side* of the *top figure*. Although material is also flowing away from the nose of the ICME sheath in the *right side* of the *top figure*, the width is expanding faster than the azimuthal speed of the flow, leading to SW accretion in the sheath. Figures from Siscoe and Odstrcil (2008). Reproduced by permission of AGU.

(2014) successfully applied a bow shock model to a FW Halo CME, but they concluded that the driven shock could be either a piston-driven shock or a bow shock. Lee *et al.* (2017) compared gas dynamic *versus* MHD models using bow shock theory to match observed stand-off distance ratios and found MHD theory more suitable for 18 limb CMEs of $W > 60°$. Kwon and Vourlidas (2017) used two models to do 3D reconstructions of three fast CME flux ropes with widths from 58° to 91° and concluded that their shocks could be piston-driven or bow shocks, depending on the local expansion of the CME. In their extended analysis of two of those CMEs to derive the shock compression ratios (Kwon and Vourlidas, 2018), they found bow-type shocks at the noses, but shocks at the flanks were freely propagating as blast waves. Thus, it has not been *a priori* obvious from observed CME W values which model provides a better description. Our observational results suggest, however, that FN CMEs are mostly bow shocks and FW CMEs predominately expansion shocks. We also have to

remember that the widths of many FW CMEs reported in the LASCO catalogs include both the CME drivers and the shock envelopes.

Shocks have also been observed ahead of relatively narrow CMEs. Vourlidas *et al.* (2003) simulated an observed shock ahead of a fast ($V_{\rm CME} = 1068$ km s^{-1}) jet-CME that maintained a narrow ($\sim 20°$) width out to 30 $R_{\rm o}$. That CME had a filamentary structure, but not the characteristic loop–cavity–core structure of broader CMEs. They showed four more (their Figure 8) examples of narrow CMEs with preceding bow-like shocks. Expanding on those results, Vourlidas and Ontiveros (2009) suggested that the bow shock morphology was associated almost exclusively with narrow CMEs.

Since FN CMEs seem likely to form bow shocks, we can ask whether those bow shocks can also produce SEP events, as do the FW CME shocks. The obvious counterpart is the Earth's bow shock, which is a stationary reverse shock with speed and density jumps of a factor of four, compared with ICME foreward shock jumps of very small to four (Richardson, 2008). Planetary bow shocks have electron and ion foreshock regions in which reflected particles can travel upstream along the magnetic field rather than being convected into the magnetosheath (Russell, 2005). Mason, Mazur, and von Rosenvinge (1996) detected short duration enhancements of heavy ions in the $\sim 30-150$ keV nuc^{-1} range upstream of the bow shock with the EPACT instrument on *Wind*. An EPACT survey (Desai *et al.*, 2000) of 1225 upstream events with durations of 10 min to 3 hours revealed steep ($\gamma = 3-4$) power-law energy spectra in the 30 to 300 keV nuc^{-1} energy range, with the bow shock source predominately quasi-parallel regions. Relatively efficient acceleration regions called hot flow anomalies have been reported (Turner *et al.*, 2018) in which first-order Fermi acceleration of ions up to 1 MeV occurs. The basic point is that the Earth's well observed strong bow shock in the SW is capable of accelerating energetic ions only to ≤ 1 MeV nuc^{-1}, in contrast to up to GeV energies in FW CME-driven shocks (Desai and Burgess, 2008). If FN CMEs also generate bow shocks in the SW, then production of E > 10 MeV SEP events would also seem unlikely.

Even if FN CMEs produce bow shocks and ~ 1 MeV nuc^{-1} energetic ions, the narrow ($\leq 60°$) injection regions might still require magnetically well located sources for those SEPs to be detected at Earth. A recent search (Bronarska *et al.*, 2018) for low energy ($E \leq 1$ MeV) particles from a sample set of 125 fast ($V_{\rm CME} > 400$ km s^{-1}) and narrow ($W < 20°$) frontside CMEs with position angles from 255° to 285° yielded 24 hits. However, the high associations of those events with type III bursts (21 of 24) and with ^{3}He-rich events (20 of 24) suggests that those authors were detecting impulsive SEP events produced in coronal reconnection events rather than by CME-driven shock acceleration. Earlier, Wang *et al.* (2012) found CMEs to be associated with most of their ^{3}He-rich events, the majority of which were narrow ($W < 50°$). We conclude that there is not yet any evidence that SEP events have been produced in bow shocks driven by FN CMEs. A possible limiting factor is the particle acceleration time scale τ, given in Equation 78 of Schwadron *et al.* (2015) as $\tau = L/V_{sz}$, where L is the shock accelerator region size and V_{sz} is the convection speed with which the magnetic flux bundles move across the shock accelerator. This term should be minimal for FN CMEs, with both small L and fast V_{sz} combining to limit the acceleration times τ.

4. Conclusions

We have done associations of fast ($V_{\rm CME} \geq 900$ km s^{-1}) with metric type II bursts and $E > 10$-MeV SEP events. We confirm earlier results that essentially no CMEs with

$W \leq 60°$, *i.e.*, the FN CMEs, are associated with either the type II bursts or SEP events. We interpret these results in terms of a distinction between bow shocks around FN CMEs and piston-driven shocks around FW CMEs. The CME-driven bow shocks are capable of producing only low energy (< 1 MeV) ions, as demonstrated by observations at the Earth's bow shock. The fundamental difference between the two is whether the SW sheath material readily flows around the propagating CME or is trapped between the shock and CME and accumulates during CME propagation. Why the cut-off seems to occur rather sharply at $W = 60°$ is not understood.

Acknowledgements S. Kahler was funded by AFOSR Task 2301RDZ4. A. Ling was supported by AFRL contract FA9453-15-C-0050. CME data were taken from the CDAW LASCO catalog. This CME catalog is generated and maintained at the CDAW Data Center by NASA and The Catholic University of America in cooperation with the Naval Research Laboratory. SOHO is a project of international cooperation between ESA and NASA. Reviewer comments improved the paper.

Disclosure of Potential Conflicts of Interest The authors declare that they have no conflicts of interest.

References

Bronarska, K., Wheatland, M.S., Gopalswamy, N., Michalek, G.: 2018, Very narrow coronal mass ejections producing solar energetic particles. *Astron. Astrophys.* **619**, A34. DOI.

Cargill, P.J.: 2004, On the aerodynamic drag force acting on interplanetary coronal mass ejections. *Sol. Phys.* **221**, 135. DOI.

Cargill, P.J., Schmidt, J.M.: 2002, Modelling interplanetary CMEs using magnetohydrodynamic simulations. *Ann. Geophys.* **20**, 879. DOI.

Desai, M.I., Burgess, D.: 2008, Particle acceleration at coronal mass ejection-driven interplanetary shocks and the Earth's bow shock. *J. Geophys. Res. Space Phys.* **113**, A00B06. DOI.

Desai, M.I., Mason, G.M., Dwyer, J.R., Mazur, J.E., von Rosenvinge, T.T., Lepping, R.P.: 2000, Characteristics of energetic ($\geq$ 30 keV/nucleon) ions observed by the Wind/STEP instrument upstream of the Earth's bow shock. *J. Geophys. Res.* **105**, 61. DOI.

Dierckxsens, M., Tziotziou, K., Dalla, S., Patsou, I., Marsch, M.S., Crosby, N.B.: 2015, Relationship between solar energetic particles and properties of flares and CMEs: statistical analysis of solar cycle 23 events. *Sol. Phys.* **290**, 841. DOI.

Dumbović, M., Čalogović, J., Vršnak, B., Temmer, M., Mays, M.L., Veronig, A.: 2018, The drag-based ensemble model (DBEM) for coronal mass ejection propagation. *Astrophys. J.* **854**, 180. DOI.

Evans, R.M., Opher, M., Manchester, W.B., Gombosi, T.I. IV: 2008, Alfvén profile in the lower corona: implications for shock formation. *Astrophys. J.* **687**, 1355. DOI.

Gopalswamy, N.: 2008, Type II radio emission and solar energetic particle events. In: *Particle Acceleration and Transport in the Heliosphere and Beyond: 7th Annual Internat. Astrophys. Conf.*, *AIP Conf. Proc.* **1039**, 196. DOI.

Gopalswamy, N., Yashiro, S.: 2011, The strength and radial profile of the coronal magnetic field from the standoff distance of a coronal mass ejection-driven shock. *Astrophys. J. Lett.* **736**, L17. DOI.

Gopalswamy, N., Lara, A., Kaiser, M.L., Bougeret, J.-L.: 2001a, Near-Sun and near-Earth manifestations of solar eruptions. *J. Geophys. Res.* **106**, 25,261. DOI.

Gopalswamy, N., Yashiro, S., Kaiser, M.L., Howard, R.A., Bougeret, J.-L.: 2001b, Characteristics of coronal mass ejections associated with long-wavelength type II radio bursts. *J. Geophys. Res.* **106**, 29219. DOI.

Gopalswamy, N., Yashiro, S., Lara, A., Kaiser, M.L., Thompson, B.J., Gallagher, P.T., Howard, R.A.: 2003, Large solar energetic particle events of cycle 23: a global view. *Geophys. Res. Lett.* **30**, 8015. DOI.

Gopalswamy, N., Aguilar-Rodriguez, E., Yashiro, S., Nunes, S., Kaiser, M.L., Howard, R.A.: 2005, Type II radio bursts and energetic solar eruptions. *J. Geophys. Res.* **110**, A12S07. DOI.

Gopalswamy, N., Yashiro, S., Xie, H., Akiyama, S., Aguillar-Rodriguez, E., Kaiser, M.L., Howard, R.A., Bougeret, J.-L.: 2008a, Radio-quiet fast and wide coronal mass ejections. *Astrophys. J.* **674**, 560. DOI.

Gopalswamy, N., Yashiro, S., Akiyama, S., Mäkelä, P., Xie, H., Kaiser, M.L., Howard, R.A., Bougeret, J.L.: 2008b, Coronal mass ejections, type II radio bursts, and solar energetic particle events in the SOHO era. *Ann. Geophys.* **26**, 1033. DOI.

Gopalswamy, N., Yashiro, S., Michalek, G., Stenborg, G., Vourlidas, A., Freeland, S., Howard, R.: 2009a, The SOHO/LASCO CME catalog. *Earth Moon Planet* **104**, 295. DOI.

Gopalswamy, N., Dal Lago, A., Yashiro, S., Akiyama, S.: 2009b, The expansion and radial speeds of coronal mass ejections. *Cent. Eur. Astrophys. Bull.* **33**, 115.

Gopalswamy, N., Akiyama, S., Yashiro, S., Mäkelä, P.: 2010, Coronal mass ejections from sunspot and non-sunspot regions. In: Hasan, S.S., Rutten, R.J. (eds.) *Magnetic Coupling between the Interior and Atmosphere of the Sun*, *Astrophys. Space Sci. Proc.*, Springer, Berlin, 289. DOI.

Guhathakurta, M., Sittler, E.C., McComas, D.: 1999, Semi-empirical MHD model of the solar wind and its comparison with ULYSSES. *Space Sci. Rev.* **87**, 199. DOI.

Guidice, D.A.: 1979, Sagamore Hill Radio Observatory, Air Force Geophysics Laboratory, Hanscom Air Force Base, Massachusetts 01731. *Report., Bull. Am. Astron. Soc.* **11**, 311.

Kahler, S.W.: 2013, A comparison of solar energetic particle event timescales with properties of associated coronal mass ejections. *Astrophys. J.* **769**, 110. DOI.

Kahler, S., Gopalswamy, N.: 2009, *CME Geometry and the Production of Shocks and SEP Events*. http://icrc2009.uni.lodz.pl/proc/pdf/icrc0266.pdf.

Kahler, S.W., Ling, A.G.: 2019, Suprathermal ion backgrounds of solar energetic particle events. *Astrophys. J.* **872**, 89. DOI.

Kahler, S.W., Reames, D.V.: 2003, Solar energetic particle production by coronal mass ejection-driven shocks in solar fast-wind regions. *Astrophys. J.* **584**, 1063. DOI.

Kahler, S.W., Reames, D.V., Sheeley, N.R. Jr.: 2001, Coronal mass ejections associated with impulsive solar energetic particle. *Astrophys. J.* **562**, 558. DOI.

Kahler, S.W., Vourlidas, A.: 2005, Fast coronal mass ejection environments and the production of solar energetic particle events. *J. Geophys. Res.* **110**, A12S01. DOI.

Kwon, R.-Y., Vourlidas, A.: 2017, Investigating the wave nature of the outer envelope of halo coronal mass ejections. *Astrophys. J.* **836**, 246. DOI.

Kwon, R.-Y., Vourlidas, A.: 2018, The density compression ratio of shock fronts associated with coronal mass ejections. *J. Space Weather Space Clim.* **8**, A08. DOI.

Kwon, R.-Y., Zhang, J., Olmedo, O.: 2014, New insights into the physical nature of coronal mass ejections and associated shock waves within the framework of the three-dimensional structure. *Astrophys. J.* **794**, 148. DOI.

Labrum, N.R.: 1972, The Culgoora Solar Radio Observatory. *Sol. Phys.* **27**, 496. DOI.

Lee, J.-O., Moon, Y.-J., Lee, J.-Y., Lee, K.-S., Kim, S., Lee, K.: 2014, Are the faint structures ahead of solar coronal mass ejections real signatures of driven shocks? *Astrophys. J. Lett.* **796**, L16. DOI.

Lee, J.-O., Moon, Y.-J., Lee, J.-Y., Kim, R.-S., Cho, K.-S.: 2017, Which bow shock theory, gasdynamic or magnetohydrodynamic, better explains CME stand-off distance ratios from LASCO-C2 observations? *Astrophys. J.* **838**, 70. DOI.

Mann, G., Klassen, A., Aurass, H., Classen, H.-T.: 2003, Formation and development of shock waves in the solar corona and the near-Sun interplanetary space. *Astron. Astrophys.* **400**, 329. DOI.

Mason, G.M., Mazur, J.E., von Rosenvinge, T.T.: 1996, Energetic heavy ions observed upstream of the Earth's bow shock by the STEP/EPACT instrument on WIND. *Geophys. Res. Lett.* **23**, 1231. DOI.

Miteva, R., Klein, K.-L., Malandraki, O., Dorrian, G.: 2013, Solar energetic particle events in the 23rd solar cycle: interplanetary magnetic field configuration and statistical relationship with flares and CMEs. *Sol. Phys.* **282**, 579. DOI.

Ontiveros, V., Vourlidas, A.: 2009, Quantitative measurements of coronal mass ejection-driven shocks from LASCO observations. *Astrophys. J.* **693**, 267. DOI.

Park, J., Moon, Y.-J., Gopalswamy, N.: 2012, Dependence of solar proton events on their associated activities: coronal mass ejection parameters. *J. Geophys. Res., Space Phys.* **117**, A08108. DOI.

Reames, D.V.: 2000, Particle acceleration by CME-driven shock waves. In: Dingus, B.L., Kieda, D.B., Salamon, M.H. (eds.) *ICRC XXVI, Invited, Rapporteur, and Highlight Papers*, *AIP Conf. Proc.* **516**, 289.

Reames, D.V.: 2013, The two sources of solar energetic particles. *Space Sci. Rev.* **175**, 53.

Reames, D.V.: 2017, *Solar Energetic Particles: A Modern Primer on Understanding Sources, Acceleration and Propagation*, *Lecture Notes in Physics* **932**, Springer, Berlin 978. DOI.

Richardson, J.D.: 2008, Flows and obstacles in the heliosphere. In: *Universal Heliophysical Processes*, *Proc. IAU Symp.* **257**, 577. DOI.

Richardson, I.G., von Rosenvinge, T.T., Cane, H.V., Christian, E.R., Cohen, C.M., Labrador, A.W.: 2014, $>$ 25 MeV proton events observed by the high energy telescopes on the STEREO a and b spacecraft and/or at Earth during the first $\sim$ seven years of the STEREO mission. *Sol. Phys.* **289**, 3059. DOI.

Robbrecht, E., Berghmans, D., Van der Linden, R.A.M.: 2009, Automated LASCO CME catalog for solar cycle 23: are CMEs scale invariant? *Astrophys. J.* **691**, 1222. DOI.

Russell, C.T.: 2005, An introduction to the physics of collisionless shocks. In: Li, G., Zank, G.P., Russell, C.T. (eds.) *The Physics of Collisionless Shocks: 4th Ann. IGPP Internat. Astrophys. Conf.*, *AIP Conf. Proc.* **781**, 3. DOI.

Russell, C.T., Jian, L.: 2008, Flows and obstacles in the solar wind. *Adv. Space Res.* **41**, 1177. DOI.

Russell, C.T., Mulligan, T.: 2002a, The true dimensions of interplanetary coronal mass ejections. *Adv. Space Res.* **29**, 301. DOI.

Russell, C.T., Mulligan, T.: 2002b, On the magnetosheath thicknesses of interplanetary coronal mass ejections. *Planet. Space Sci.* **50**, 527. DOI.

Schmelz, J.T., Reames, D.V., von Steiger, R., Basu, S.: 2012, Composition of the solar corona, solar wind, and solar energetic particles. *Astrophys. J.* **755**, 33. DOI.

Schwadron, N.A., Lee, M.A., Gorby, M., Lugaz, N., Spence, H.E., Desai, M.: 2015, Particle acceleration at low coronal compression regions and shocks. *Astrophys. J.* **810**, 97. DOI.

Siscoe, G., Odstrcil, D.: 2008, Ways in which ICME sheaths differ from magnetosheaths. *J. Geophys. Res.* **113**, A00B07. DOI.

Takahashi, T., Mizuno, Y., Shibata, K.: 2016, Scaling relations in coronal mass ejections and energetic proton events associated with solar superflares. *Astrophys. J. Lett.* **833**, L8. DOI.

Takahashi, T., Shibata, K.: 2017, Sheath-accumulating propagation of interplanetary coronal mass ejection. *Astrophys. J. Lett.* **837**, L17. DOI.

Tappin, S.J.: 2006, The deceleration of an interplanetary transient from the Sun to 5 Au. *Sol. Phys.* **233**, 233. DOI.

Turner, D.L., Wilson, L.B., Liu, T.Z., Cohen, I.J., Schwartz, S.J., Osmane, A.: 2018, Autogenous and efficient acceleration of energetic ions upstream of Earth's bow shock. *Nature* **561**, 206. DOI.

Vourlidas, A., Ontiveros, V.: 2009, Review of coronagraphic observations of shocks driven by coronal mass ejections. In: *Shock Waves in Space & Astrophysical Environments: 18th Ann. Internat. Astrophys. Conf.*, *AIP Conf. Proc.* **1183**, 139. DOI.

Vourlidas, A., Wu, S.T., Wang, A.H., Subramanian, P., Howard, R.A.: 2003, Direct detection of a coronal mass ejection-associated shock in large angle and spectrometric coronagraph experiment white-light images. *Astrophys. J.* **598**, 1392. DOI.

Vršnak, B., Cliver, E.W.: 2008, Origin of coronal shock waves. *Invited Review, Sol. Phys.* **253**, 215. DOI.

Vršnak, B., Vrbanec, D., Čalogovi, J.: 2008, Dynamics of coronal mass ejections. The mass-scaling of the aerodynamic drag. *Astron. Astrophys.* **490**, 811. DOI.

Vršnak, B., Ružđjak, D., Sudar, D., Gopalswamy, N.: 2004, Kinematics of coronal mass ejections between 2 and 30 solar radii. What can be learned about forces governing the eruption? *Astron. Astrophys.* **423**, 717. DOI.

Wang, L., Lin, R.P., Krucker, S., Mason, G.M.: 2012, A statistical study of solar electron events over one solar cycle. *Astrophys. J.* **759**, 69. DOI.

Webb, D.F., Howard, T.A.: 2012, Coronal mass ejections: observations. *Living Rev. Solar Phys.* **9**, 3. DOI.

Yashiro, S., Michalek, G., Gopalswamy, N.: 2008, A comparison of coronal mass ejections identified by manual and automatic methods. *Ann. Geophys.* **26**, 3103. DOI.

Žic, T., Vršnak, B., Temmer, M., Jacobs, C.: 2008, Cylindrical and spherical pistons as drivers of MHD shocks. *Sol. Phys.* **253**, 237. DOI.